Proceedings of 20th International Congress on Acoustics, ICA 2010

23–27 August 2010, Sydney, Australia

Sonic crystal noise barriers made of resonant elements

A. Krynkin (1), O. Umnova (1), A.Y.B. Chong (2), S. Taherzadeh (2) and K. Attenborough (2)

(1) Acoustics Research Centre, The University of Salford, Salford, Greater Manchester, UK

(2) Department of Design Development Environment and Materials, The Open University, Milton Keynes, UK

PACS: 43.20.Fn, 43.20.Ks, 43.40.Fz, 43.50.Gf

ABSTRACT

The main spectral property of a Sonic Crystal structure is a notable sound attenuation related to the Bragg band gaps. This effect is observed in air and makes Sonic Crystals effective noise barriers in a particular frequency range. This performance can be extended to a wider range of frequencies by introducing scatterers supporting multiple resonances of various types. In this paper the sonic crystals composed of infinitely long multi-resonant composite scatterers are studied. First the concentric elastic shell and outer 4-slit rigid cylinder composite is considered. Theoretical and experimental results show the existence of the axisymmetric resonance of the elastic shell followed by the annular cavity resonance. The second type of scatterers considered is a U-shaped resonator composed of thin elastic plates. The plates form an open cavity so that resonances are defined by their bending motion as well as by the geometry of the scatterer. Theoretical analysis of the elastic-acoustic coupling in a single scatterer is based on the Kirchhoff-Love asymptotic theory. Numerical results on the overall performance of the proposed structures are obtained with the multiple scattering technique and finite element method. The predictions are compared with the experimental results.

INTRODUCTION

One of the distinctive features of finite periodic arrays of scatterers is the high attenuation over the selective range of frequency intervals [1, 2]. This effect is explained by the theory of wave propagation in the infinite periodic structures [3]. In these structures there exist the band gaps where waves do not propagate. It is well-known that the band gaps can be tuned to the selected frequencies by changing the spacing between scatterers that can significantly improve the performance of the periodic structure as the acoustic screens.

There are many different approaches on how to improve the performance of the periodic structures such as increasing the filling fraction [4], varying the arrangement of the scatterers [5] and replacing scatterers by the resonant elements [6, 7, 8]. Own resonances of the array elements create standing waves that result in the existence of new low frequency band gaps along with the classical Bragg band gaps [9]. In this paper we propose two different resonant elements such as concentric N-slit cylinder and thin elastic shell and U-shaped scatterer with elastic walls, referred to as composites.

Resonant properties of thin elastic structures in air, such as shells and plates, are being analysed using Kirchhoff-Love approximations. Using this preliminary results the elastic materials can be chosen so that resonances appear at low frequencies. The elastic shells and plates form a part of the composites, which exhibit additional resonances related to the constructed cavity. When composite elements are arranged in doubly-periodic arrays, these resonances generate band gaps.

The first type of resonators preserves axisymmetric resonance of the elastic shell although it appears at a lower frequency. Additional resonance due to the annular cavity and the slits is observed at a higher frequency. This resonant behaviour is predicted by solving semi-analytically scattering problem for the proposed concentric composite (array of composites). To solve this problem the multiple scattering technique [2] and approach in modeling gratings [11] are used. The predictions are then compared with the experimental results.

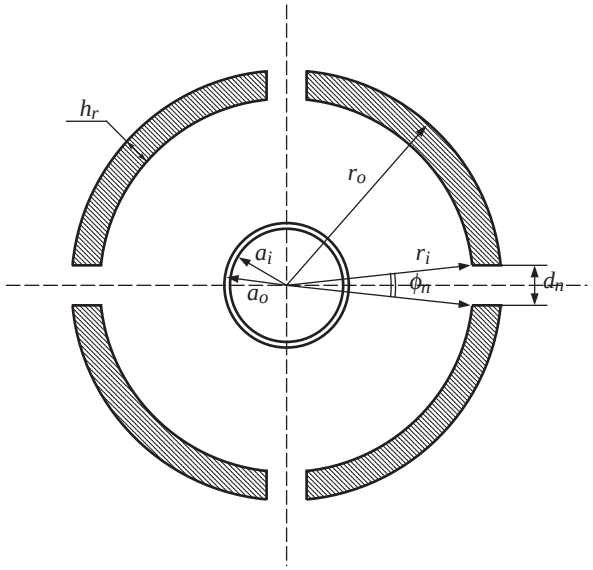

Figure 1: Cross-section of composite scatterer consisting of concentric arrangement of a hollow 4-slit rigid cylinder and an inner elastic cylindrical shell.

The second type of the resonating elements is represented by the U-shaped scatterer composed of the elastic plates. The results are obtained with finite element method (COMSOL Multiphysics 3.4) for single U-shaped resonator as well as for the array of such scatterers.

CONCENTRIC N-SLIT CYLINDER AND ELASTIC SHELL

Auxiliary problem. Single scatterer

Consider two-dimensional problem of acoustic wave scattering by a single N-slit rigid cylindrical shell of thickness h_r and of external radius r_o in air ($\rho = 1.25\,\mathrm{kg/m^3}$ and $c = 344\,\mathrm{m/s}$). The sound is generated by the cylindrical point source placed at the origin of the Cartesian (x,y)/Polar (r,θ) coordinate system. The width of consecutive slits in Oxy plane is denoted as d_n, $n = 1..N$ and they are infinitely long in the direction of the cylinder main axis Oz, see Figure 1(a). It is also assumed that the thickness of the rigid cylinder is much smaller than its radius $h_r/r_o \ll 1$.

The N-slit cylinder is concentrically arranged with thin elastic shell of external radius a_o and half thickness h. The physical parameters of the shell are given by density ρ_s, the compressional c_1 and shear c_2 wave speeds. The wave field outside of the composite is described by acoustic potential $p(\boldsymbol{r})$ that is the solution of the Helmholtz equation

$$\Delta p + k^2 p = 0, \tag{1}$$

and subject to the Somerfeld's radiation conditions

$$\frac{\partial p}{\partial r} - ikp = o\left(r^{-1/2}\right), \text{ as } r \to \infty, \tag{2}$$

where $r = \sqrt{x^2+y^2}$, $k = \omega/c$ is the ratio between angular frequency and sound speed of the acoustic environment and Laplacian Δ is given by either $\frac{1}{r}\frac{\partial}{\partial r}\left(r\frac{\partial}{\partial r}\right) + \frac{1}{r^2}\frac{\partial^2}{\partial\theta^2}$ or $\frac{\partial^2}{\partial x^2} + \frac{\partial^2}{\partial y^2}$.

The scattering problem formulated only for the elastic shell surrounded by the acoustic environment (i.e. air) can be analysed by using Kirchhoff-Love approximations. Provided that thickness of the shell is much smaller than its mid-radius $R = (a_o + a_i)/2$ (i.e. $h/R \ll 1$) we can derive simple analytical form of the solution in the outer acoustic environment that satisfies equation (1) and continuity conditions imposed on the surface of the shell. This solution is given by [8]

$$p(r,\theta) = H_0^{(1)}(kr) + \sum_{n=-\infty}^{+\infty} A_n Z_n H_n^{(1)}(k\hat{r})\exp(in\hat{\theta}),\ \hat{r} > a_o, \tag{3}$$

where

$$Z_n = \frac{J_n'(kR)}{H_n^{(1)'}(kR) + i\hat{U}_{1,n}}, \tag{4}$$

with

$$\begin{aligned} \hat{U}_{1,n} &= \frac{\varepsilon}{\kappa_o}\frac{n^2 - k_3^2R^2}{\pi Rh\left(1 + n^2 - k_3^2R^2\right)J_n'(kR)}, \\ k_3 &= \frac{\omega}{c_3}, \quad c_3 = \sqrt{\frac{E}{\rho\left(1-\nu^2\right)}}, \\ \varepsilon &= \frac{\rho c}{\rho_s c_2}, \quad \kappa_o = \frac{c}{c_2}. \end{aligned} \tag{5}$$

Using this solution we can find insertion loss at the point of observation in the following form

$$IL = 20\log_{10}\left|\frac{H_0^{(1)}(kr)}{p}\right|, \tag{6}$$

Figure 2(a) illustrates results obtained for the single shell made of latex with $E = E(\omega)$ and $\nu = 0.4997$ [8]. We must note that

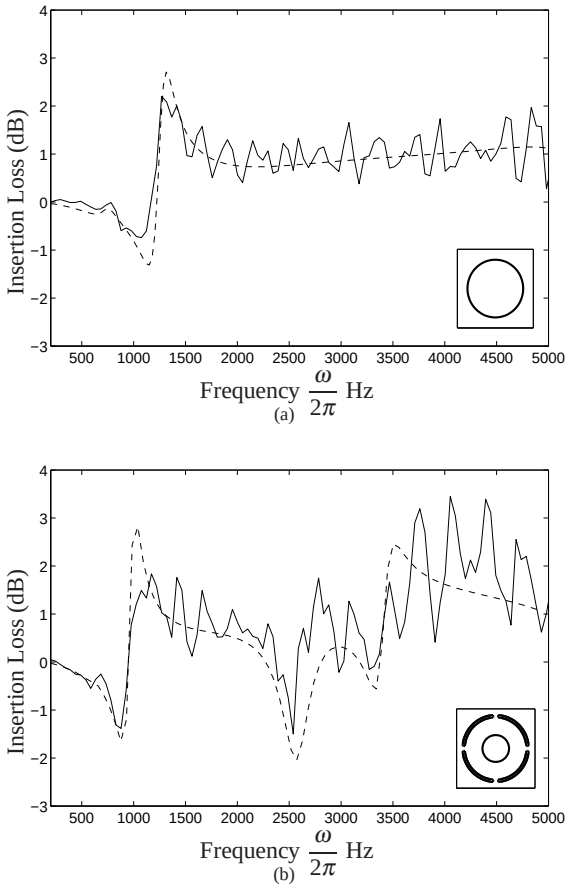

Figure 2: Insertion loss computed analytically (- - - -) and measured experimentally (———) for single scatterer. Distances from scatterer to the source and receiver are 1.5 m and 0.05 m, respectively. (a) The viscoelastic shell made of latex ($a_o = 0.0215$ m and $h = 0.00025$ m). (b) Concentric 4-slit rigid cylinder ($r_o = 0.0275$ m, thickness $h_r = 0.002$ m and $d_n = 0.004$) and viscoelastic shell made of latex ($a_o = 0.0215$ m and $h = 0.00025$ m).

to introduce viscosity the general form of Young's modulus is dependent on ω in the following form

$$E(\omega) = E - \sum_{j=1}^{N}\frac{i\omega\tau_j E_j}{(1 - i\omega\tau_j)}, \tag{7}$$

where Young's modulus E related to the equilibrium state is always set to 1.75 MPa and dynamic moduli E_j and relaxation times τ_j are taken from [10]. In this plot the axisymmetric resonance of the elastic shell (i.e. $n = 0$) is observed at around 1300 Hz. This resonance is followed by the resonance of the index $n = 1$ which is found at around 800 Hz.

For scattering problem by the concentric N-slit rigid cylinder and elastic shell the solution of the elastic shell has to be coupled with the solutions found inside the slits and outside/inside of the rigid cylinder. In doing so we first derive boundary conditions imposed on the surface of N-slit cylinder in the following form [11]

$$\begin{aligned} \frac{\partial p_i}{\partial r} &= \frac{\partial p_o}{\partial r} + f(\theta)k^2 h_r p_o, \\ \frac{\partial p_o}{\partial r} &- \frac{f(\theta)}{h_r}(p_o - p_i) = 0, \end{aligned} \tag{8}$$

where p_o and p_i are the solutions of equation (1) at $r = r_o, r_i$ and $f(\theta)$ is the piecewise function setting the boundary condi-

tions at the slit faces. In this paper we consider the case of four symmetrically distributed identical slits (i.e. $N=4$ and $\phi_n=\phi$) that corresponds to

$$f(\theta)=\sum_{n=2}^{N}\left\{H\left(\theta-\frac{2\pi(n-1)}{N}+\frac{\phi}{2}\right)-H\left(\theta-\frac{2\pi(n-1)}{N}-\frac{\phi}{2}\right)\right\}+\sum_{j=0}^{1}\left\{H\left(\theta-2\pi j+\frac{\phi}{2}\right)-H\left(\theta-2\pi j-\frac{\phi}{2}\right)\right\}, \quad (9)$$

The inner product $\int_0^{2\pi} <\cdot> e^{-im\theta}d\theta$, $m\in\mathbb{Z}$, transforms boundary conditions (8) into the following algebraic system of equations in A_m, $m\in\mathbb{Z}$, variables

$$\sum_{n=-\infty}^{\infty}A_n\left\{\delta_{m,n}2\pi hH_n^{(1)'}(kr_o)-F_{n-m}\left[H_n^{(1)}(kr_o)-H_n^{(1)'}(kr_o)I_n\right]+\frac{k^2h}{2\pi}H_n^{(1)}(kr_o)\sum_{j=-\infty}^{\infty}F_{j-m}F_{n-j}I_j\right\}= \quad (10)$$

$$\sum_{n=-\infty}^{\infty}H_n^{(1)}(kQ)e^{-in(\pi+\alpha)}\left\{-\delta_{m,n}2\pi hJ_n'(kr_o)+F_{n-m}\left[J_n(kr_o)-J_n'(kr_o)I_n\right]-\frac{k^2h}{2\pi}J_n(kr_o)\sum_{j=-\infty}^{\infty}F_{j-m}F_{n-j}I_j\right\},\ m\in\mathbb{Z},$$

where $\delta_{m,n}$ is Kronecker delta, vector $\boldsymbol{Q}=Q(\cos\alpha,\sin\alpha)$ is the radius vector to the centre of the protector and

$$I_n=\frac{J_n(kr_i)+\mathscr{C}_nY_n(kr_i)}{J_n'(kr_i)+\mathscr{C}_nY_n'(kr_i)}, \quad (11)$$

$$F_n=\begin{cases}N\phi & \text{for}\quad n=0,\\ \dfrac{2\sin(n\phi/2)}{n}\displaystyle\sum_{l=0}^{N-1}e^{-2in\pi l/N} & \text{for}\quad n\neq 0,\end{cases} \quad (12)$$

with $\mathscr{C}_n$ defining the concentric elastic shell as

$$\mathscr{C}_n=0, \qquad \text{no elastic shell,} \quad (13)$$

$$\mathscr{C}_n=-\frac{J_n'(kR)}{Y_n'(kR)+\hat{U}_{1,n}}, \qquad \text{elastic shell.} \quad (14)$$

To find numerical solution, infinite system of equations (10) is truncated at $m=-30..30$ that gives results accurate to three significant figures. Knowing the coefficients A_n the insertion loss (6) can be found through the outer solution written as

$$p_o=H_0^{(1)}(k_or)+\sum_{n=-\infty}^{+\infty}A_nH_n^{(1)}(k\hat{r})e^{in\hat{\theta}}, \quad (15)$$

Figure 2(b) shows the insertion loss derived for the concentrically arranged thin elastic shell and 4-slit rigid cylinder. The resonant behaviour of the concentric elastic shell (related to the axisymmetric resonance) is observed around 1000 Hz. By comparing this results with those in Figure 2(a) it is seen that this resonance is shifted towards lower frequency by approximately 300 Hz. This shift is explained by the coupling of two resonators that are elastic shell and 4-slit cylinder. In Figure 2(b) we can also identify resonances above 2000 Hz that are related to the Helmholtz resonator and the annular cavity formed by surfaces of concentric elements.

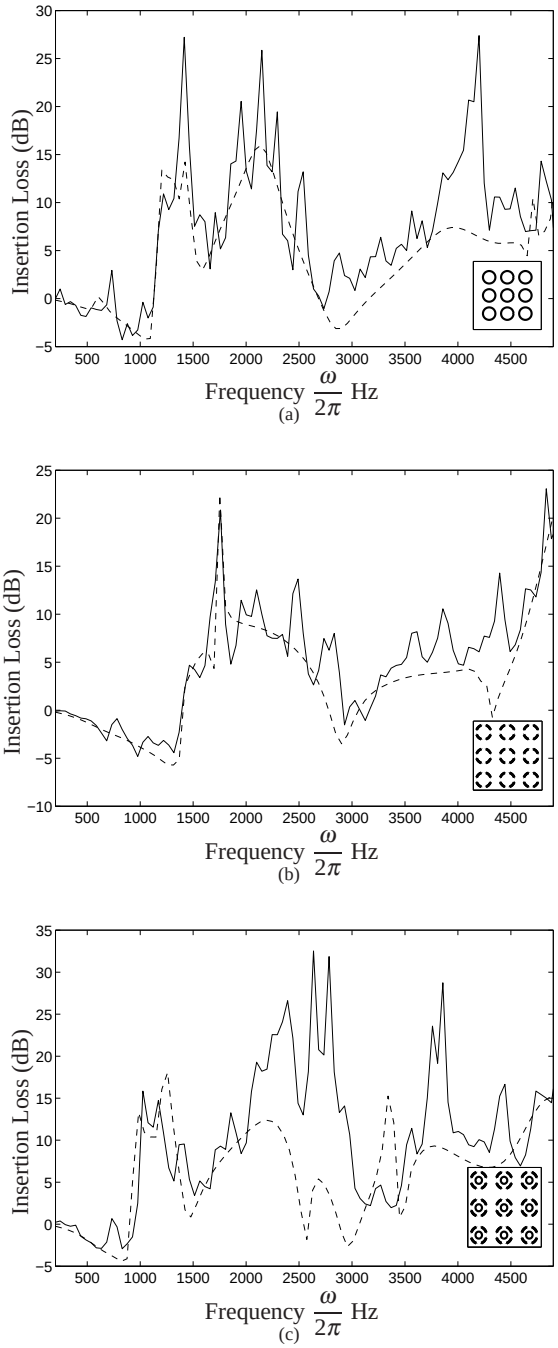

Figure 3: Insertion loss (6) computed analytically (- - - -) with (16) and measured experimentally (———) for square 3x3 array of scatterers with lattice constant $L=0.08$ m. Distances from scatterer to the source and receiver are 1.5 m and 0.05 m, respectively. (a) The viscoelastic shell made of latex ($a_o=0.0215$ m and $h=0.00025$ m). (b) 4-slit rigid cylinder ($r_o=0.0275$ m, thickness $h_r=0.002$ m and $d_n=0.004$). (c) Concentric 4-slit rigid cylinder ($r_o=0.0275$ m, thickness $h_r=0.002$ m and $d_n=0.004$) and viscoelastic shell made of latex ($a_o=0.0215$ m and $h=0.00025$ m).

Array of scatterers

We next consider finite periodic array of $\mathcal{N}$ scatterers. Using multiple scattering technique [2] the infinite system of equations in A_m^p, $p = 1..\mathcal{N}$, $m \in \mathbb{Z}$, variables is derived as

$$\sum_{n=-\infty}^{\infty} A_n^p \left\{ \delta_{m,n} 2\pi h H_n^{(1)\prime}(kr_{o,p}) - F_{n-m}^p \left[H_n^{(1)}(kr_{o,p}) - H_n^{(1)\prime}(kr_{o,p}) I_n^p \right] + \frac{k^2 h}{2\pi} H_n^{(1)}(kr_{o,p}) \sum_{j=-\infty}^{\infty} F_{j-m}^p F_{n-j}^p I_j^p \right\}$$
$$+ \sum_{s=1, s\neq p}^{\mathcal{N}} \sum_{n=-\infty}^{\infty} \sum_{v=-\infty}^{\infty} A_n^s H_{n-v}^{(1)}(kQ_{ps}) e^{-i(n-v)(\pi+\alpha_{ps})} \left\{ \delta_{m,v} 2\pi h J_n'(kr_{o,p}) - F_{v-m}^p \left[J_n(kr_{o,p}) - J_n'(kr_{o,p}) I_n^p \right] + \frac{k^2 h}{2\pi} J_v(kr_{o,p}) \sum_{j=-\infty}^{\infty} F_{j-m}^p F_{v-j}^p I_j^p \right\} = \quad (16)$$
$$\sum_{n=-\infty}^{\infty} H_n^{(1)}(kQ_p) e^{-in(\pi+\alpha_p)} \left\{ -\delta_{m,n} 2\pi h J_n'(kr_{o,p}) + F_{n-m}^p \left[J_n(kr_{o,p}) - J_n'(kr_{o,p}) I_n^p \right] - \frac{k^2 h}{2\pi} J_n(kr_{o,p}) \sum_{j=-\infty}^{\infty} F_{j-m}^p F_{n-j}^p I_j^p \right\},$$
$$m \in \mathbb{Z},\ p = 1..\mathcal{N},$$

where A_m^p are the unknown coefficient of the solution of equation (1) given by

$$p_o(r,\theta) = H_0^{(1)}(kr) + \sum_{m=1}^{\mathcal{N}} \sum_{n=-\infty}^{+\infty} A_n^m H_n^{(1)}(k\hat{r}_m) e^{in\hat{\theta}_m}, \quad (17)$$

vector $\boldsymbol{Q}_m = Q_m(\cos\alpha_m, \sin\alpha_m)$ is the radius vector to the centre of m-th scatterer, $\boldsymbol{Q}_{mp} = Q_{mp}(\cos\alpha_{mp}, \sin\alpha_{mp})$ are the coordinates of p-th scatterer with respect to m-th scatterer, $(\hat{r}_m(r,\theta), \hat{\theta}_m(r,\theta))$ are the polar coordinates with origin at the centre of m-th scatterer and factors I_m^p and F_m^p are given by equations (11) and (12), respectively.

Figure 3 illustrates the performance of the finite square array made of the resonant elements. The Bragg band gap is observed around 2100 Hz. Below this frequency the elastic shell resonances are identified by the maxima of the insertion loss in Figure 3(a) and (c). As seen in Figure 3(a) the strongest effect is achieved for the axisymmetric resonance around 1300 Hz for the array of elastic shells. In Figure 3(c), plotted for the array of concentric 4-slit cylinders and elastic shells, the insertion loss maximum is shifted to 1000 Hz. This effect is related to the shift of the axisymmetric resonance described in the previous section. Figure 3(b) demonstrates the acoustic effects predicted with (16) and observed experimentally for the array of 4-slit rigid cylinders. One can see positive insertion loss peak around the Helmholtz resonance 1500 Hz followed by Bragg band gaps at 2100 and 4200 Hz and cavity resonance around 4900 Hz.

U-SHAPED RESONATORS

Auxiliary problem. Single scatterer

In this section we consider scattering by a single U-shaped resonator surrounded by air. The resonator is formed by two parallel elastic beams attached to the rigid backing, see Figure 4. This scatterer may support the resonances of the elastic beam

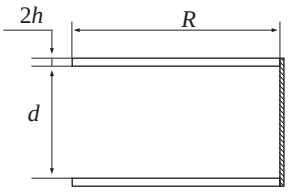

Figure 4: Cross-section of composite scatterer made of U-shaped cavity with elastic walls and rigid backing. d=0.02 m, R=0.07 m, h=0.004 m

(see Table 1) as well as the resonances of the open cavity. In the low-frequency range (wavelength λ is much bigger than width of the cavity d) and provided that R is much bigger than d the first cavity resonance can be approximated by [12]

$$f = \frac{c}{4R} \quad (18)$$

Table 1:
Solution of equation
$\cosh\left(R(3k_3^2/h^2)^{1/4}\right)\cos\left(R(3k_3^2/h^2)^{1/4}\right) + 1 = 0$

Material	Frequency Hz		
Polyethylene	137	858	2401
Steel	690	4324	12109

The results are obtained by using finite element method implemented in COMSOL Multiphysics 3.4. In the numerical model the outer acoustic environment is surrounded by the perfectly matched layer (PML). It is also assumed that sound is generated by the incident plane wave that is taken as exp(-ikx). These assumptions allow us to narrow down the active domain in Comsol model to array-receiver distance and, as a result, to reduce the computational time.

Figure 5 illustrates insertion loss computed for the elastic and rigid U-shaped scatterers. In Figure 5(a) elastic beams are made of polyethylene. It can be seen that the second resonance of the elastic beam at $f \approx 850$ Hz is followed by the first cavity resonance. This resonance is slightly shifted towards higher frequencies compared to that of the rigid cavity whose first resonance is approximated by equation (18). The observed effect of coupling of resonances is analogous to that of the concentrically arranged 4-slit cylinder and elastic shell. The performance of the steel resonator shown in Figure 5(b) has little difference with that of the rigid scatterer. Nevertheless one can observe the appearance of first resonance of the steel beam at $f \approx 690$ Hz.

Array of scatterers

The resonators whose performance is analysed in the previous section can now be used in constructing the finite array. The distance between the centres of the scatterers in the array is 0.08 m and the scatterers are arranged in a finite square lattice. As before the incident plane wave propagates parallel to Ox axis.

In Figure 6 the performance of the finite array is analysed. Figure 6(a) illustrates the existence of the band gap around $f \approx$ 850 Hz related to the resonance of the elastic beam made of polyethylene. The second positive insertion loss peak around $f \approx 1150$ Hz is generated by the first cavity resonance. Due to the low filling fraction (approximately 9%) the first Bragg band gap does not contribute to the positive performance of the array. The insertion loss of the array of steel resonators shown in Figure 6(b) is similar to that of the rigid resonator array. As

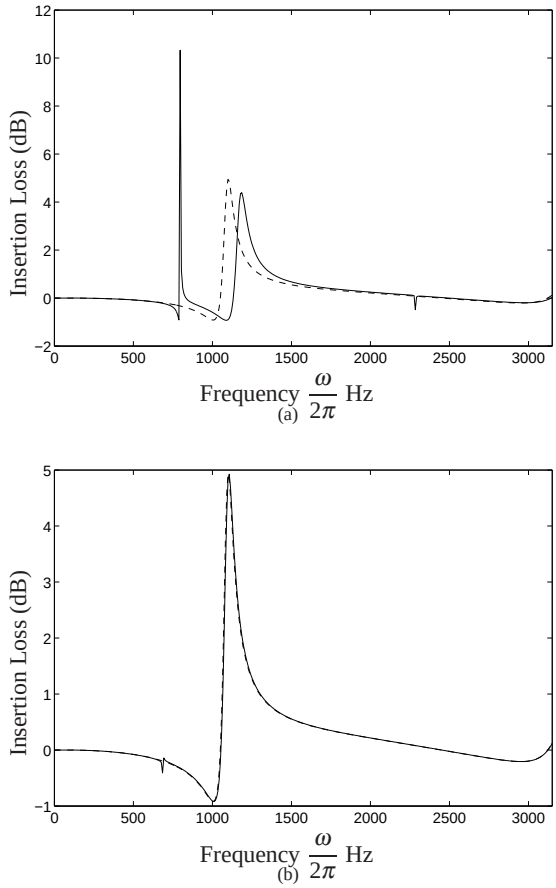

Figure 5: Insertion loss (6) computed numerically for U-shaped scatterer made of either elastic (———) or rigid (- - - -) walls. Distance from scatterer to receiver is 0.05 m. (a) Polyethylene elastic walls. (b) Steel elastic walls.

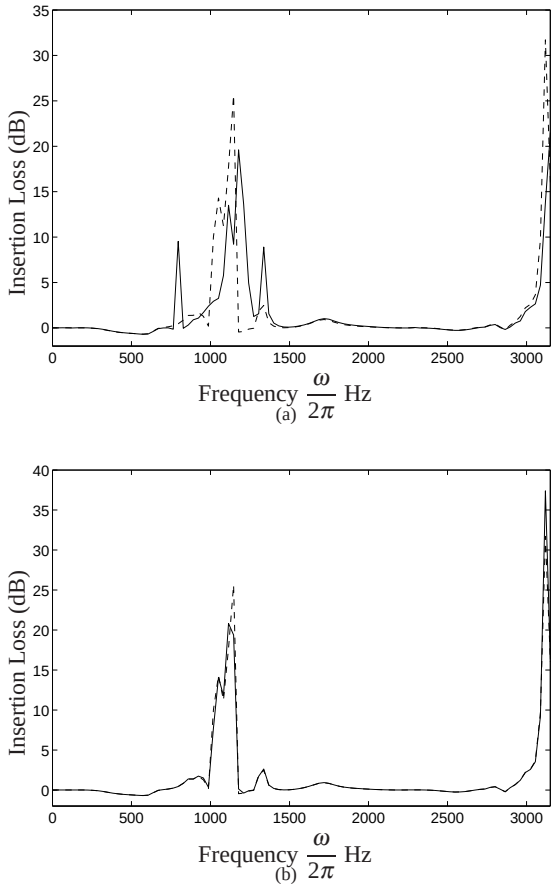

Figure 6: Insertion loss (6) computed numerically for 7x3 array of U-shaped scatterers made of either elastic (———) or rigid (- - - -) walls. Distance from scatterer to receiver is 0.05 m. (a) Polyethylene elastic walls. (b) Steel elastic walls.

can be seen the structural vibration excited in the steel beam is weak so that it does not contribute into the scattererd wave field in the acoustic medium.

CONCLUSION

The use of the resonating elements in Sonic Crystals results in effective sound attenuation in the low-frequency range while still preserving the existence of the Bragg band gaps. The composite scatterer made of resonators supports resonances characterised by both structural and air born vibrations. The coupling between these vibrations results in shift of the resonances corresponding to each element of the composite, the effect that is observed in the mass-spring system with multiple degree of freedom.

ACKNOWLEDGMENTS

This work was supported by the EPSRC research grants EP/E063136/1 and EP/E062806/1. Authors are grateful for this support. AK is grateful to the International Commission for Acoustics for the award of a Young Scientist Conference Attendance Grants.

REFERENCES

[1] Miyashita, T., Sonic crystals and sonic wave-guides, Measurement Science and Technology, **16**, 47–63 (2005).

[2] Umnova, O., Attenborough, K. and Linton, C.M., Effects of porous covering on sound attenuation by periodic arrays of cylinders, The Journal of the Acoustical Society of America, **119**, 278–284 (2006).

[3] Movchan, A.B., Movchan, N.V. and Poulton, C.G., *Asymptotic Models of Fields in Dilute and Densely Packed Composites*, Imperial College Press, 2002.

[4] Caballero, D., Sanchez-Dehesa, J., Rubio, C., Martinez-Sala, R., Sanchez-Perez, J. V., Meseguer, F. and and Llinares, J., Large two-dimensional sonic band gaps, Physical Review E, **60**(1999), R6316–R6319

[5] Romero-Garcia, V., Fuster, E., Garcia-Raffi, L. M., Sanchez-Perez, E. A., Sopena, M., Llinares, J. and Sanchez-Perez, J. V., Band gap creation using quasiordered structures based on sonic crystals, Applied Physics Letters, **88**(2006), 174104.

[6] Sainidou, R., Djafari-Rouhani, B., Pennec, Y. and Vasseur, J.O., Locally resonant phononic crystals made of hollow spheres or cylinders, Physical Review B, **73**, 024302 (2006).

[7] Cui, Z.Y., Chen, T.N., Chen, H.L. and Su, Y.P., Experimental and calculated research on a large band gap constituting of tubes with periodic narrow slits, Applied Acoustics, **70**, 1087–1093 (2009).

[8] Krynkin, A., Umnova, O., Chong, A.Y.B., Taherzadeh, S. and Attenborough, K., Predictions and measurements of sound transmission through a periodic array of elastic

shells in air, Journal of the Acoustical Society of America, submitted.

[9] Movchan, A.B. and Guenneau, S., Split ring resonators and localized modes, *Physical Review B*, **70**(2004), 125116.

[10] Merheb, B., Deymier, P.A., Jain, M., Aloshyna-Lesuffleur, M., Mohanty, S., Berker, A. and Greger, R.W., Elastic and viscoelastic effects in rubber/air acoustics band gap structures: A theoretical and experimental study, Journal of Applied Physics, **104**(2008), 064913.

[11] Montiel, F. and Neviere, M., Perfectly conducting gratings: a new approach using infinitely thin strips, Optics Communications, 144(1997), 82–88.

[12] Morse, P.M. and Ingard, K.U., *Theoretical Acoustics*, Princeton University Press, 1986.